Chinese Journal of Mechanical Engineering

REVIEW   **Open Access**

Chip Formation Mechanism of Inconel 718: A Review of Models and Approaches

Chun Liu[1,2], Min Wan[1,2]*, Weihong Zhang[1,2] and Yun Yang[1,2]

Abstract

Inconel 718, a nickel, chrome and iron alloy, has special advantages, such as high-temperature strength, thermal resistance and corrosion resistance, which facilitate wide usage in the aerospace industry, especially in the hot sections of gas turbine engines. However, machining this alloy is correlated closely with the material's inherent properties such as excellent combination of strength, hardness and toughness, low thermal conductivity and the tendency to adhere to cutting tools. This nickel alloy also contains inclusions of hard abrasive carbide particles that lead to work-hardening of the workpiece material and thus abrasive wear of the cutting tool. That is, the machining of Inconel 718 is always influenced by high mechanical and thermal loads. This article reviews the chip formation mechanism of Inconel 718. One of the main characteristics in machining of Inconel 718 is that it will produce serrated or segmented chips in a wide range of cutting speeds and feeds. Existing studies show that the chip serration or segmentation by shear localization affects the machined surface integrity, and also contributes to the chip's evacuation and the automation of machining operations. Thus, research conclusion indicates that the serrated or segmented chip phenomenon is desirable in reducing the level of cutting force, and detailed analysis of models and approaches to understand the chip formation mechanism of Inconel 718 is vital for machining this alloy effectively and efficiently. Therefore, this article presents some summaries on the models and approaches on the chip formation in machining of Inconel 718.

Keywords: Inconel 718, Chip formation mechanism, Shear instability, Segmented chip

1 Introduction

Nickel-based superalloys (Ni, Fe-Ni, Co base), which are further subdivided into wrought, cast and powder metallurgy alloys [1, 2], were initially created in the 1940s [3]. Owing to the properties and features that are competent for the extreme working conditions, e.g., the excellent mechanical strength, the superb resistance to surface degradation and the good oxidation resistance even at elevated temperatures [4–6], these alloys outperform many other metals and alloys [1]. Thus, up to 45%–50% (weight percentage) of materials used in machining an aircraft engine (mainly the gas turbines) are nickel-based superalloys [7]. Nickel alloys are also used in rocket engines, space vehicles, nuclear reactors, submarines and other applications involving high temperatures above 550 ℃ [6, 8]. Besides, another factor, which has helped these nickel alloys enter the aerospace industry, is the competition basically from military companies to achieve excellent engines with a higher power and performance, but meanwhile possessing a minimized weight [8].

Among the nickel alloys, Inconel 718 accounts for about 45% of wrought nickel-based products and 25% of cast nickel-based products [9], and it is widely employed as critical components such as vanes, discs and liners. Since the 1960s, Inconel 718 has been emerged as a standard nickel alloy due to its high-temperature strength, excellent mechanical properties and outstanding corrosion resistance produced at relatively low costs [10]. Therefore, some articles were published on the machining performance of Inconel 718 over the last few decades [2, 4]. However, Inconel 718 is

*Correspondence: m.wan@nwpu.edu.cn
[1] School of Mechanical Engineering, Northwestern Polytechnical University, Xi'an 710072, China
Full list of author information is available at the end of the article

Liu *et al. Chin. J. Mech. Eng.*   (2021) 34:34

Page 2 of 16

considered as one of the most difficult-to-cut materials. The mainly poor machinability properties are as follows [1, 4, 8, 11, 12]: (1) strong tendency to form built-up edge (BUE), (2) work-hardening behaviors leading to high cutting force, (3) rapid tool wear due to hard abrasive carbide particles, (4) strength retention at elevated temperatures, (5) low thermal conductivity leading to high cutting temperature, and (6) high hardness. All of these properties make nickel-based superalloys extremely difficult to satisfy the quality and production requirements. Just because of these inherent characteristics, machining Inconel 718 leads to many technical and economic problems. As a result, the alloy's milling, drilling and turning were carried out at relatively low cutting speeds and feeds compared to the machining process of other alloys like steel and aluminum. Therefore, practical machining of Inconel 718 usually needs more time and higher cost.
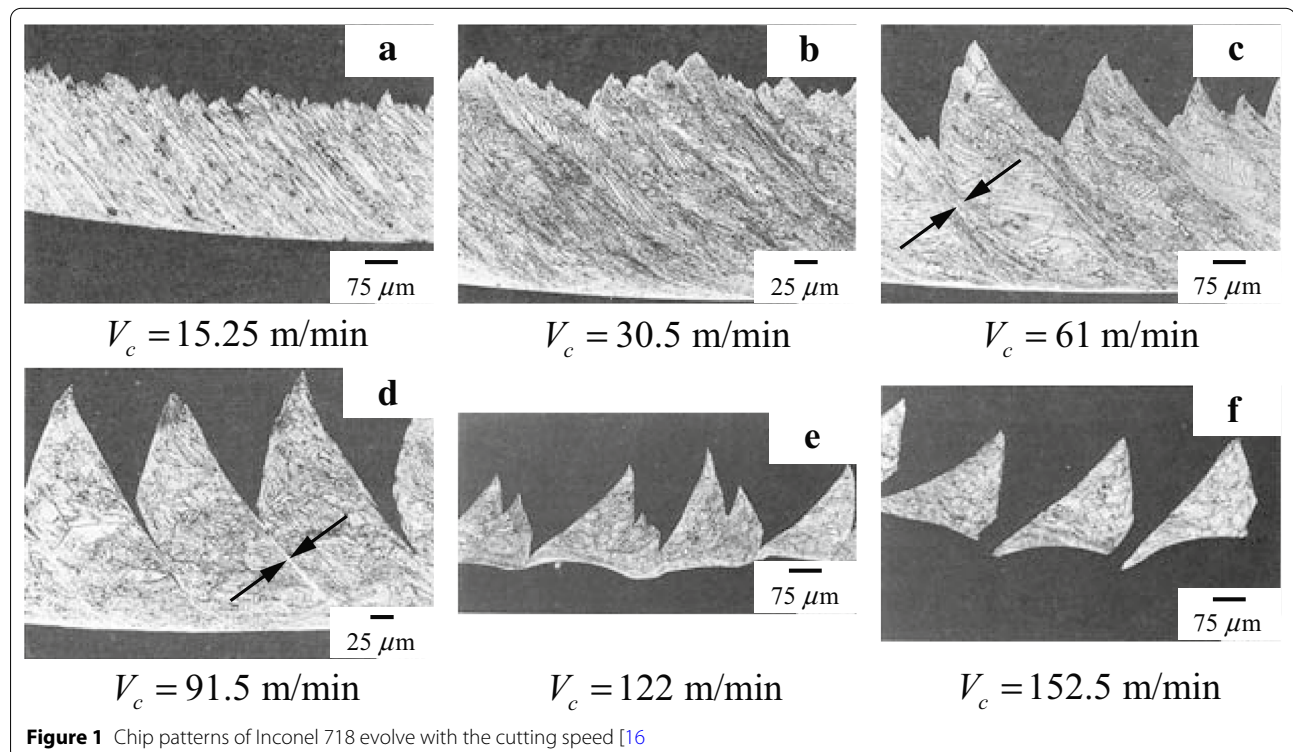
Better understanding of chip formation mechanism plays an important role in machining process planning, surface integrity improvement and thus product performance [13, 14]. In consideration of its significance, researches on chip formation mechanism under different cutting conditions are indispensable to a deep insight of the whole cutting process [15]. Therefore, an effort to have a thorough understanding of the chip formation mechanism in machining of Inconel 718 is great necessary, and it is reviewed in this article.

2 Machinability and Associated Problems
2.1 Characteristics and Types of Chip
The chip morphology of Inconel 718 usually depends on the properties of the workpiece and cutting conditions, i.e. cutting speed, feed and tool geometry [13]. Figure 1 shows the optical micrographs of Inconel 718 chip, which are related to the longitudinal midsections at various cutting speeds [16]. At relatively low cutting speeds, mechanically continuous chips can be observed (Figure 1a, b). As speed increases, the chip pattern witnesses a transition from the continuous status to a periodic serration (Figure 1a, b, c, d). The serrated chips (Figure 1c, d) are comprised of two regions, in which the deformations within the chip are grossly inhomogeneous. One is the narrow bands between the two arrows related to the neighboring segments in Figure 1c, d, in which the deformation is very high, and the other is the materials within the individual segments in Figure 1c, d, in which the deformation is relatively low [17, 18]. It is worth noting that these deformation features are also observed for other materials like titanium alloy Ti-6Al-4V [19–21] and AISI 4340 steel [22]. Therefore, the shear-localized instability happening in the primary shear zone results in the intensely

Figure 1 Chip patterns of Inconel 718 evolve with the cutting speed [16

Liu *et al. Chin. J. Mech. Eng.*   (2021) 34:34

Page 3 of 16

concentrated shear bands between neighboring segments. With the further increase of the cutting speed, the contact area between the neighboring segments decreases rapidly (Figure 1c, d, e). At still higher cutting speed, the segments within the chips are eventually separated (Figure 1e to f), i.e. the discontinuous chip is produced.

It should be mentioned that the microstructure within the adiabatic shear band evolves during the shear-localized chip formation, and these phenomena were observed by the Scanning Electron Microscope, as reported in many studies. For instance, Cai and Dai [23] pointed out that the transition from the shear localized deformation to the homogeneous deformation in cutting of Inconel 718 is not relevant to the cutting speed in the dynamic large strain extrusion machining processes. Lorentzon et al. [24] concluded that the chip segmentation in machining of the aged and forged alloy 718 shows thermal softening and material fracture. Besides Inconel 718, Wan et al. [25] summarized that the changes from the deformed band to the deformed band plus the transformed band and then to the transformed band are the microstructure evolution of adiabatic shear bands in machining of Ti-6Al-4V. Murr et al. [26] found that the adiabatic shear band evolution of Ti-6Al-4V was accompanied by the evolution of dark deformation bands composed of α' martensite platelets. Duan and Zhang [27] concluded that in high speed machining of AISI 1045 steel, low cutting speed is easy to produce the deformed adiabatic shear band, which is usually relevant to severe plastic shear, while high cutting speed can lead to the transformed adiabatic shear band, which involves recrystallization, reorientation and elongation of the martensite laths.

From the cross sections shown in Figure 1, it can be seen that there are mainly two types of chip morphology for Inconel 718, i.e., the continuous chip and the cyclically serrated chip. For the continuous pattern (Figure 1a, b), the chips appear to be uniform in the direction of thickness. In this case, a long chip tends to be formed. Thus, control methods should be taken to prevent chip accumulation around the cutting region. However, for the serrated pattern (Figure 1c, d), the non-uniformity in the direction of thickness is very clear. Specifically, the thin shear bands within the serrated chips are alternately separated by large bulk of segments [16]. This feature may result from the dynamic response of the machine-tool structure, shear localized deformation in the chip, or fracture within the chip [28]. Generally, the continuous chip formation occurs under relatively low cutting speeds and feeds, while the serrated chips, which are also called "the segmented chip", "the saw-tooth chip" and "the shear-localized chip", are produced at high cutting speeds and feeds. Apart from the chip patterns mentioned above, there are other subcategories. For instance, Komanduri and Brown [29], and Vyas and Shaw [30] subdivided chips into the following types, i.e., the continuous ribbon, the shear-localized chip, the segmented chip, the chip with BUE, the wavy chip and the discontinuous chip.

2.2 Associated Problems

One of the main limitations restricting the wide use of Inconel 718 is the conventional type of machining. On the one hand, this alloy has excellent resistance qualities, while on the other hand, they make it much less suitable for machining [31]. Actually, many factors such as the workpiece material, the type of cutting operation, the cutting tool used, etc., affects the actual cutting speed and feed. However, with technology progressing, the cutting efficiency has improved. For instance, according to the Refs. [32, 33], the range of high speed in machining of nickel-based superalloys was more than 50 m/min, but later, as experimentally reported in Ref. [34], the cutting speeds of the nickel-based superalloys Inconel 718 can reach up to 2100 m/min by using computer-controlled lathe and light-gas gun based device.

As mentioned in Figure 1, the chip morphology of Inconel 718 changes greatly under different conditions. The continuous chips indicate the steady-state of cutting process, while the cyclically serrated chips imply the instable cutting. At low cutting speeds and feeds, the chip control is poor because of its continuous ribbon-type morphology [14] that may get entangled. At high cutting speeds and feeds, the chips mostly tend to be continuous but with abrasive saw-tooth edges at the free side. Effects of the segmented chip on cutting process of Inconel 718 have been extensively investigated. Although the serrated chip by shear localization is easy to break, chip segmentation also affects cutting force, temperature and surface finish quality, and leads to rapid tool wear. For instance, Liu et al. [35] found that the periodical change of mechanical and thermal loadings affects the segmentation of the chip in orthogonal machining of Inconel 718. Sun et al. [36] observed a cyclic force during the segmented chip formation in dry turning of Ti-6Al-4V. Agmell et al. [37] also observed that the serrated chip of AISI 316L leads to periodic change of cutting force, which in turn has a drastic effect on the mechanical stresses of the cutting tool. Su et al. [38] found that micro-waves on the machined surface in cutting of alloy steel AerMet 100 were caused by the chip serration. Mabrouki et al. [39] also found that the segmentation periodicity can lead to the appearance of waved machined surface.

Liu *et al. Chin. J. Mech. Eng.*   (2021) 34:34

Page 4 of 16

On the one hand, the shear-localized chip or the other types of the periodically serrated chip are desirable from the respect of chip disposal [28], and it contributes to the automation of machining operations and other applications involving chip recycling. On the other hand, the intensity of chip serration increases with cutting speed. At high cutting speeds, intense shear takes place so rapidly that the contact between neighboring segments reduces and tends to vanish until the discontinuous chips are formed [17]. This instability causes fluctuation of cutting force and thus vibration or even chatter [40] in the metal cutting process, which limit the material removal rate, degrade the surface finish and reduce the tool life [28, 41–44]. For these reasons, a number of researchers have investigated the formation mechanism of chips to seek a balanced solution. Recht [45] firstly recognized the localized shear as a process of "catastrophic thermoplastic shear" due to the softening of materials within the shear zones. Specifically, shear localization tends to occur when thermal softening effects outweigh the strain and strain rate hardening effects. From this work, Recht [45] ranked the affinity of different metals towards shear localization, but the transition of the critical cutting speed of the chip pattern from the continuous chip to the shear-localized chip was not focused. Lately, Komanduri et al. [19, 20, 22] and Turley et al. [46] performed similar work on various alloys such as AISI 4340 steel and titanium alloy Ti-6Al-4V. The contribution of their work gives a good explain for the mechanism of shear-localized chip flow.

It is mentioned in Figure 1 that the plastic deformation in the chip formation region in machining of Inconel 718 is inhomogeneous. Highly localized deformations are involved in the chip ahead of the cutting tool, and the intensely concentrated shear bands appear. Due to the low thermal conductivity, all generated heats are concentrated within these narrow bands, and thus, they dramatically increase the local temperature in the chip formation region.

Therefore, it must be emphasized that the mechanism of chip formation governs the extent of tool wear, magnitudes of the cutting force and the temperature, and the machined surface integrity [47]. But, it is impractical to experimentally investigate the nature of machining performance related to Inconel 718 in a large range of cutting conditions, due to the time-consuming, laborious and expensive process. To overcome these disadvantages, employing new cutting methods is one way that can give favorable help. The other is to establish analytical and numerical models, and seek an insight into the kernel of the problem that thus contributes to predict and optimize the cutting process.

2.3 New Cutting Methods

Compared with conventional-type machining, new methods, which are mainly the ultra-high speed machining, ultrasonic vibration-assisted machining and grinding, are employed to help cut Inconel 718 and other difficult-to-cut materials. Thus, the cutting performance improves and exhibits a distinct feature, which relates to the chip formation process.

For the ultra-high speed machining, Ye et al. [34] experimentally investigated the evolution patterns of the chip in cutting of Inconel 718 by varying the cutting speed from 0.05 m/s to 35.78 m/s, and established an expression to characterize the critical cutting speed for the generation of the serrated chip flow. Except this paper, articles on ultra-high speed machining of Inconel 718 are very limited, and many studies were mainly focused on the chip formation in ultra-high speed machining of other difficult-to-cut materials. For instance, Ye et al. [48] observed that in the cutting speed range from 0.05 m/s to 31.2 m/s, the continuous chip can be transformed to the serrated form in the machining of titanium alloy Ti-6Al-4V. Based on a specific ballistic set-up, Sutter and List [49] found that in cutting of Ti-6Al-4V, the serrated chip can be transformed to another discontinuous pattern when the cutting speed varies from 300 m/min to 4400 m/min. Through analyzing the formation of the segmented chip, Gente et al. [50] observed the microstructure change of Ti-6Al-4V at extremely high cutting speeds, i.e., from 300 m/min to 6000 m/min. With respect to AISI 1045 steel, Ye et al. [51] observed that as the cutting speed changes from 30.8 m/s to 67.3 m/s, the continuous chip can be transformed to the saw-tooth chip.

Ultrasonic vibration-assisted machining can offer distinct advantages compared to the conventional machining methods for different materials including Inconel 718. For instance, Babitsky et al. [52] found that chip formation in ultrasonic vibration-assisted turning of Inconel 718 is more regular, and it produces continuous chips with small serrations. This phenomenon was also confirmed by the reports in Refs. [53, 54]. Besides Inconel 718, Muhammad et al. [55] realized generating shorter chips in the machining of $\alpha + \beta$ titanium alloy by adopting the ultrasonically assisted turning. Ni et al. [56] and Ibrahim et al. [57] obtained shorter, thinner and smoother chips in the ultrasonic vibration-assisted milling of titanium alloy Ti-6Al-4V.

Besides, it should be noted that grinding is another special machining process widely used to improve the surface quality and accuracy. This process contributes to chip evacuation and small force even for difficult-to-cut materials like nickel alloys. For instance, Patil et al. [58] obtained ample short strained chips and debris in deep

Liu *et al. Chin. J. Mech. Eng.*   (2021) 34:34

Page 5 of 16

grinding of Inconel 718 with cBN wheel at the high speed of 180 m/s. Li et al. [59] observed flow chips rather than shear chips in ultrasonic assisted grinding of Inconel 718. Zhao et al. [60] found that there existed cracks and segments in the chips produced from the high speed grinding of Inconel 718 with single grain. Besides Inconel 718, Peng et al. [61] obtained continuously smooth and thin chips in the vertical elliptic ultrasonic vibration-assisted grinding of brittle polysilicon. Tesfay et al. [62] experimentally obtained thin, smooth and short chips in the ultrasonic vibration-assisted grinding of bio-ceramics. Kitzig-Frank et al. [63] found chipping around the produced scratch in the ultrasonic-assisted grinding of Alumina.

3 Analytical Models

Investigations on the chip formation mechanism in machining are basically by experimental measurements and numerical analyses. However, the chip formation mechanism related to Inconel 718 is different from that of steels, copper and aluminum [17] because of its distinct properties. As cutting speed increases, an obvious change of chip pattern of Inconel 718 is observed. That is, a continuous chip (Figure 2) at relatively low cutting speeds and feeds will transform to a serrated pattern (Figure 3) once high cutting speeds and feeds are adopted. As long as the localized shears are initiated, and penetrate through the whole chip thickness, the chip's free side will become saw-teeth shape. The higher the cutting speed, the larger the intensity of chip serration [64]. It should be mentioned that the serrated chips are easy to
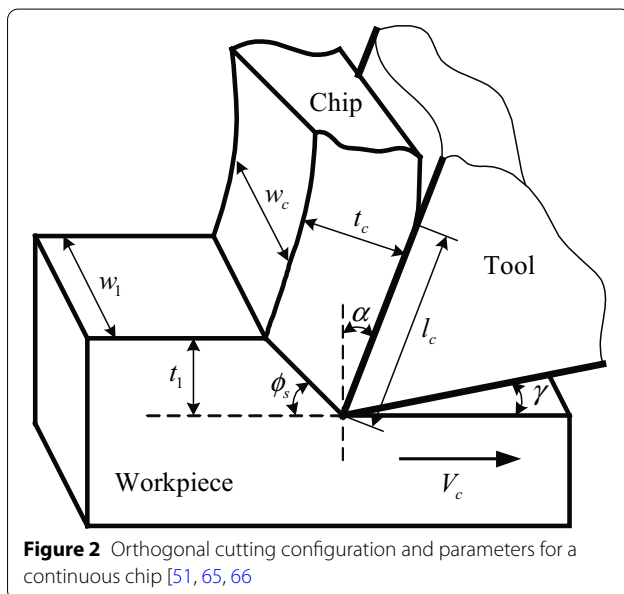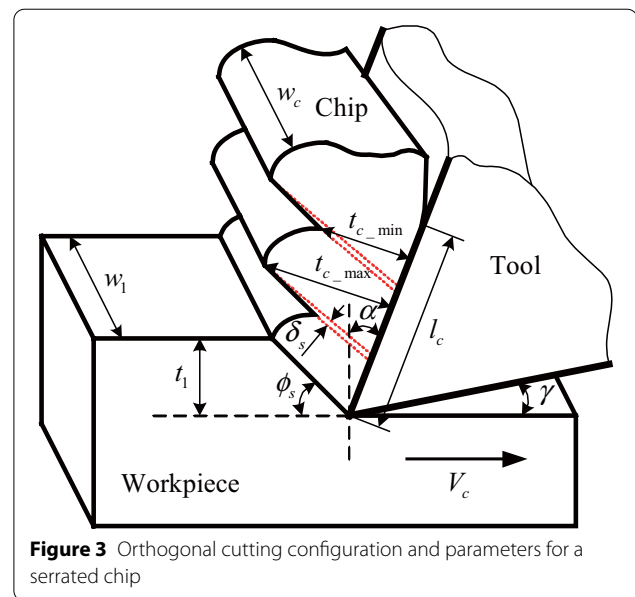

Figure 3 Orthogonal cutting configuration and parameters for a serrated chip

break. Therefore, establishing good models to capture the details of the transition of chip patterns is especially significant for the optimization of the cutting process [24]. Where in Figures 2 and 3, V_c is cutting speed, t_1 is undeformed chip thickness, t_c is chip thickness, w_1 is width of cut, w_c is width of chip, ϕ_s is shear angle, α is tool rake angle, γ is tool clearance angle, l_c is chip-tool contact length, t_{c_max} is maximum chip thickness, t_{c_min} is minimum chip thickness, δ_s is shear band thickness.

As reported in Refs. [16, 19, 20], two stages can be summarized to describe the process of the serrated chip formation in machining of Inconel 718. At the first stage, the strain localization and the plastic instability both occur in the chip formation region, due to the catastrophic shear failure along the shear surface. Then a new shear band, which originates from the tool tip, is formed. The new shear band will gradually propagate and concavely curve upwards until it meets the chip's free surface. At the other stage, gradual bulging of the workpiece material ahead of the cutting tool takes place and will result in a saw-tooth. Generally, the highly concentrated shear bands observed between the neighboring segments are actually formed in this stage [22].

However, focuses are placed on the investigation of the continuous chip formation due to the relatively stable cutting process. Moreover, it is commonly asserted that continuous chips are produced under the conventional cutting conditions [64]. But at high cutting speeds, the narrow shear-localized bands are formed due to the plastic instability. The method for describing a serrated chip deformation is different from that used to calculate the deformation for a continuous chip [67]. To model the

Figure 2 Orthogonal cutting configuration and parameters for a continuous chip [51, 65, 66]

Liu *et al. Chin. J. Mech. Eng.*   (2021) 34:34

Page 6 of 16

serrated chip formation at high cutting speeds, the following three assumptions are made.

(1) Plain strain deformation happens within the workpiece material.
(2) The workpiece material is isotropic, consecutive and incompressible.
(3) The cutting process is stable without BUE.

Figure 3 is a configuration of orthogonal cutting operation. Note that the cutting edge is vertical to the cutting speed V_c, and the chip width w_c is much larger than the chip thickness t_c. Therefore, the assumption of the plane strain is adopted. It needs to mention that the investigation of chip deformation is useful for understanding the cutting process of Inconel 718. It is necessary to establish a function between the outputs, e.g., chip morphology, cutting force and temperature, and the input parameters, e.g., cutting speed, feed and depth of cut [68]. But the primary trouble is that it needs to experimentally analyze the chip deformation characteristics in large quantities.

However, the parameters such as the chip thickness ratio t_1/t_c, the shear angle ϕ_s and the shear strain ε, which are often used to describe a continuous chip deformation, cannot fully assess the deformation of a serrated chip. Because the serrated chips are usually comprised of two different regions, i.e., the grossly inhomogeneous deformation within narrow shear bands, and the segment bulks with relatively low deformation [16].

3.1 Chip Formation Theory

Inconel 718 has an affinity to produce segmented chips at high cutting speeds. The characteristic of segmentation often leads to instable machining. Thus, a thorough understanding of the characteristic of chip segmentation is important. Generally, there are mainly two theories to explain the serrated chip formation, i.e., (i) the adiabatic shear theory and (ii) the periodic crack theory.

The first one is on the saw-tooth chip caused by the periodic thermoplastic shear instability that occurs in the chip formation region. The shear instability during the cutting process is caused at the critical point that the material softening effects outperform the combined effects of strain and strain rate hardening [19, 69]. Meanwhile, the generated heats in the shear zones exceed the heats diffusing into the environment [70]. Generally, shear localization appears once a critical shear strain occurs. This criterion for the shear instability has also been researched for the other difficult-to-cut metals such as titanium alloy and hardened steel [34]. Due to the low thermal conductivity of Inconel 718, the heats generated by the plastic deformation often accumulate
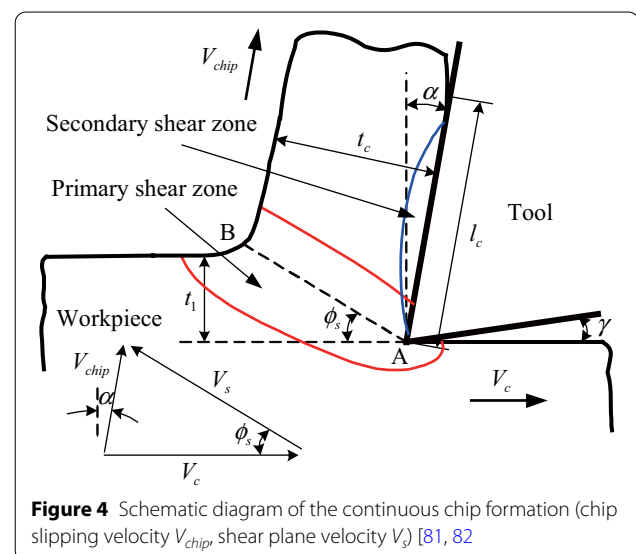
in the narrow shear-localized bands. The adiabatic shear is also referred as "localized-shear", "catastrophic shear" and "thermoplastic instability shear". Scholars of the adiabatic shear theory include Recht [45], Komanduri et al. [22], Semiatin and Rao [28], Davies et al. [42], Joshi et al. [71], Molinari et al. [72] and Sutter [66]. Furthermore, the experiment observation shows that the widths of adiabatic shear bands are from a few micrometers to a few tens of micrometers [69].
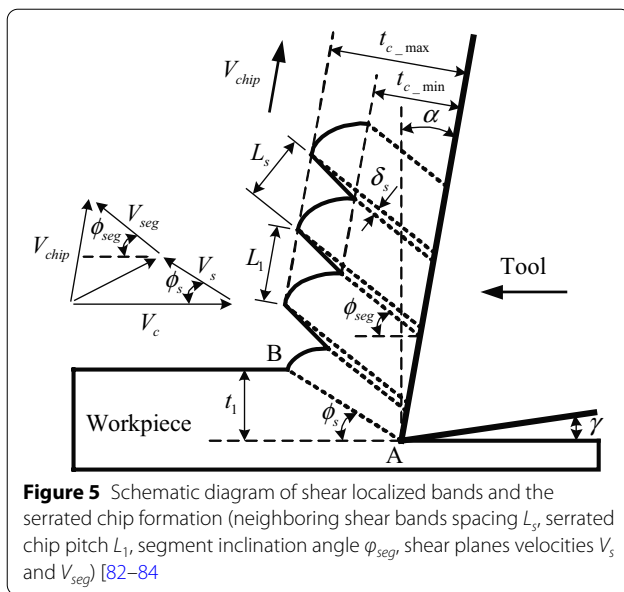
The second theory explains that the chip serration is caused by the crack initiation and propagation [30, 73], and it points out that the crack initiates from the chip's free surface and propagates towards the tool tip in the primary shear zone. It is the periodic crack that leads to the serrated chip formation. Supporters are Poulachon and Moisan [74], Elbestawi et al. [75], Shaw and Vyas [76] and Nakayama et al. [77], etc.

Researchers also combine the adiabatic shear theory with the periodic crack theory to explain the serrated chip formation since both adiabatic shear and periodic crack happen in the serrated chip formation [69, 78]. Thus, the two theories can be integrated to work as the principles for the failure of a material. Despite existing divergences, whether the slide surface of a segment is caused by adiabatic shear or periodic cracks, a common view has been achieved. That is, ductile materials tend to produce serrated chip by adiabatic shear, while brittle materials prefer periodic cracks in the serrated chip formation [79, 80].

3.2 Chip Morphology Analysis

Chip morphology analysis is a useful method to assess a material's machinability, which directly influences the

Figure 4 Schematic diagram of the continuous chip formation (chip slipping velocity V_{chip}, shear plane velocity V_s) [81, 82]

Liu *et al. Chin. J. Mech. Eng.*   (2021) 34:34

Page 7 of 16

Figure 5 Schematic diagram of shear localized bands and the serrated chip formation (neighboring shear bands spacing L_s, serrated chip pitch L_1, segment inclination angle φ_{seg}, shear planes velocities V_s and V_{seg}) [82–84]

cutting time and cost. Continuous chip shown in Figure 4 is usually produced under relatively low cutting speeds and feeds, due to the homogeneous shear occurring in the primary shear zone [28]. As cutting speed increases, Inconel 718 produces the segmented chips, as shown in Figure 5. Continuous chip represents the cutting stability process. However, the serrated or segmented chip represents the cutting instability process while the chip sliding on the tool rake face.

Shear localized bands can develop during the rapid deformation in high speed machining. Usually, it is observed that the serrated chips are continuous in appearance, but microscopically jointed together by heavily deformed narrow bands. As mentioned in the above section, the chip morphology change is mainly due to adiabatic shear and periodic crack. Researchers of adiabatic shear pointed out that insufficient heat diffusion leads to the local temperature rising and thus shear instability [66, 72], while researchers of periodic crack believed that crack initiation and propagation result in fracture damage [75, 76]. However, the transition from the continuous chip to the serrated chip was originally considered to be the thermal softening effect overcoming the work hardening effect, thus encouraging shear localization. Therefore, many articles supporting of this theory try to focus on a criterion for shear localization. For instance, Bayoumi and Xie [85] defined the chip load $V_c \times f$ (feed f) as criterion for the onset of chip serration. Zhen-Bin and Komanduri [86] proposed the critical cutting speed for the serrated chip formation. Besides to them, Recht [45] studied the critical strain rate. Xie et al. [87] suggested the flow localization parameter. Li et al.

[88] studied the material properties and deformation conditions for the onset of adiabatic shear.

Therefore, numerous attempts have been made to study the onset of the serrated chip formation in the metal cutting process. Many researchers focused on the mechanism of the serrated chip formation [21, 30, 46, 64, 72, 79]. One reason is that difficult-to-cut metals, such as nickel-based superalloys, titanium alloys and hardened steels, show similar chip pattern change during the metal cutting process at industries. Another reason is that, chip serration in high speed cutting leads to rapid tool wear and degraded surface finish. However, the positive side is that chip serration contributes to the chip evacuation and the automation of machining operations [88].

4 Computational Solution
Finite element method (FEM) has been widely employed as an useful means to simulate the metal cutting process, and it not only promotes better understanding of the cutting process, but also saves time and cost [89]. It also reduces the number of actual experiments by trial and error [90, 91]. For the last few years, many researches have been focused on the machinability of Inconel 718 [92]. It has been proved that machining Inconel 718 needs more time and higher cost because of its low machinability compared to other alloys. Therefore, simulation of the cutting of Inconel 718 by FEM is an effective way to understand the details of the chip formation mechanism [93–95].

4.1 Material Constitutive Models
The material behavior during the chip formation is the combined result of the workpiece material properties and the used cutting conditions. In the metal cutting process, large strain, high stress and high temperature usually occur, and they further affect the microscopic and macroscopic response of a material. FEM can be used to model this cutting process. The material model is the most important factor that influences the accuracy of the FEM-based simulation. A correct simulation enables good predictions, which in turn contribute to the optimization of the machining process.

The material constitutive model is usually used for the material deformation [96], which is the prerequisite for conducting finite element simulation. The accuracy of constitutive relation directly affects the accuracy of finite element simulation. The purpose of FEM simulation is to imitate the real cutting conditions, finally to predict the results to provide theoretical and technical support for improving the quality and efficiency of actual machining. Therefore, for cutting simulation, it is very important to select or establish a constitutive relationship which is related to the properties of materials.

Liu *et al. Chin. J. Mech. Eng.*   (2021) 34:34

Page 8 of 16

In FEM simulation, Inconel 718 was usually modeled as a material with elastic-plastic and isotropic hardening. The flow stress is a function of strain, strain rate and temperature [97]. The material constitutive models usually include the Johnson-Cook (JC) model [98] and its modifications [99–101], the Baummann-Chiesa-Johnson (BCJ) model [102] and the Steinberg-Cochran-Guinan (SCG) model [103]. Among them, the JC model is the most widely used. The parameters of JC constitutive equation are usually achieved by fitting the data obtained by the split Hopkinson press bar (SHPB) test under different temperatures and strain rates.

4.1.1 Johnson-Cook Constitutive Model

The Johnson-Cook (JC) constitutive equation, which is comprised of plastic strain ε, strain rate $\dot{\varepsilon}$ and temperature T, is expressed as follows [98]:

$$\sigma = \left(A + B\varepsilon^n\right)\left[1 + c\ln\left(\frac{\dot{\varepsilon}}{\dot{\varepsilon}_0}\right)\right]\left[1 - \left(\frac{T - T_r}{T_m - T_r}\right)^m\right],$$ (1)

where σ is the equivalent flow stress. ε is the equivalent plastic strain. $\dot{\varepsilon}$ is the equivalent plastic strain rate. $\dot{\varepsilon}_0$ is the reference equivalent plastic strain rate. T is the workpiece temperature. T_m and T_r are the material melting temperature and the room temperature, respectively. A, B, n, C and m are the material parameters. The parameter A is the initial yield strength of the material at room temperature. B is the hardening modulus. n is the work hardening exponent. C is the coefficient dependent on strain rate and m is the thermal softening coefficient.

It is assumed that each bracket of the JC constitutive equation is independent. The dependence of the stress with respect to the strain can be obtained by SHPB test under different strain rates and temperatures. Although JC constitutive model has been widely used in cutting simulations, there are still deficiencies. One is the limitations, which can not characterize the flow stress behavior of all materials. The other is that JC model does not consider the coupling effects of strain, strain rate and temperature. In fact, especially in high speed cutting, severe plastic deformation is accompanied by high temperature and large strain rate. Thus, the mechanical thermal coupling effect is very obvious. Therefore, in order to accurately characterize the plastic flow behavior of materials in cutting process, modifications of the basic JC constitutive model have been done [42, 99–101, 104]. It should be pointed out that other constitutive models are less used, and thus, they will not be elaborated in this review.

4.2 Chip Separation Criterion

For simulation, describing the separation between chip and workpiece matrix as close as possible to reflect the actual cutting process will directly affect the result accuracy [105]. If the separation principle is not selected properly, the simulation process may not converge or even report errors. There are two kinds of criteria to describe the separation between chip and workpiece matrix. The first kind is geometric criterion [106], which determines whether the distance between the tool tip on the cutting path and the unit node ahead of the tool tip reaches the preset critical failure value. Once the distance reaches the preset critical failure value, the node will fracture and separate into two nodes. One will continue to flow with the chip formed and the other node will remain on the machined surface. The second kind is physical criterion [107, 108], which uses the equivalent plastic strain, fracture stress, strain energy density or other physical variables as the chip separation principle. Similarly, when the physical variables at the tool tip reach the preset critical value, the unit nodes are separated.

Appropriate chip separation criterion dominates the cutting simulation. Therefore, a powerful chip separation criterion needs to be established to accurately predict the chip formation process. Generally, continuous chip formation has been considered in the development of numerical models for metal cutting. Saw-tooth chip formation has been simulated by different methods, such as the strain-based fracture criterion [109], the Johnson-Cook (JC) damage model [110, 111], the energy-based fracture criterion [112], the Baummann-Chiesa-Johnson (BCJ) model [113, 114] and the pure deformation method [115]. As for the discontinuous chip formation in simulation, the strain-based fracture criterion [116] is usually adopted.

Usually, a good criterion can exhibit the mechanics and the physical mechanism of materials, and can also give reasonable results related to the chip pattern, cutting force, temperature and residual stresses. In addition, the critical value of a sound criterion for a particular material keeps constant at different cutting conditions [117]. For instance, Strenkowski and Carroll [118] adopted the effective plastic strain as the chip separation criterion to simulate the chip formation, and found that changing the critical value of the effective plastic strain had little effect on the chip morphology and cutting force. Komvopoulos and Erpenbeck [119] found that the preset value of the distance criterion must be carefully chosen to avoid cutting instability in simulation. Lin and Lin [120] found that the strain energy density in chip separation was independent of the uncut chip thickness. Watanable and Umezu [121] used the normal failure stress as the fixed separation criterion and obtained a good correlation of cutting force and chip deformation.

Liu *et al. Chin. J. Mech. Eng.*   (2021) 34:34

Page 9 of 16

The criteria discussed above assumed that the critical damage value is a constant depending on the workpiece material, but does not depend on the cutting conditions [122]. However, these criteria have various problems in practice. For instance, there are no sound rules in determining the strain energy density, tool-node distance and effective plastic strain. Furthermore, they may be only known by experience and chosen by trial and error method [117].

4.2.1 Fractural Model
To model the separation of the chip from the workpiece matrix, the Johnson-Cook (JC) damage model [123] (shear failure) was usually used as the damage initiation criterion [10], combined with the JC constitutive model. The JC damage model is based on the equivalent plastic strain at the element integration points. It is assumed that failure occurs when the damage parameter is large than one [10]. The damage parameter is given as follows:

$$D = \sum \frac{\Delta \varepsilon}{\varepsilon_f}, \tag{2}$$

where $\Delta \varepsilon$ is the increment of equivalent plastic strain, and ε_f is the equivalent strain to fracture. The strain at fracture is given by [123]:

$$\varepsilon_f = \left[D_1 + D_2 \exp \left(D_3 \frac{\sigma_m}{\overline{\sigma}} \right) \right] \left[1 + D_4 \ln \left(\frac{\dot{\varepsilon}}{\dot{\varepsilon}_0} \right) \right] \left[1 + D_5 \left(\frac{T - T_r}{T_m - T_r} \right) \right], \tag{3}$$

where the variables $\sigma^* = \frac{\sigma_m}{\overline{\sigma}}$, $\dot{\varepsilon}^* = \frac{\dot{\varepsilon}}{\dot{\varepsilon}_0}$ and $T^* = \frac{T - T_r}{T_m - T_r}$ are constants, and the dimensionless pressure-stress ratio meets the condition of $\sigma^* \leq 1.5$. σ_m is the average of the three normal stresses, and $\overline{\sigma}$ is the von Mises equivalent stress. The dimensionless strain rate $\dot{\varepsilon}^*$ and the homologous temperature T^* are identical to those used in the strength model of the JC constitutive equation. The five constants D_1, D_2, D_3, D_4 and D_5 are the failure parameters measured at or below the transition temperature.

The first term implies the strain to fracture [124] as σ_m increases. The second term represents the effect of strain rate. The third term represents the effect of temperature. Different relationship [123] is used when $\sigma^* > 1.5$. The material is to fracture when $D = 1.0$. The JC damage equation captures the coupled effect of stress, strain rate and temperature.

According to the thermal softening theory, the flow stress will decrease once the damage initiation criterion is satisfied. The material fracture process is the evolution of damage [10]. An element will be removed from the surrounding elements once it fails, and a crack will initiate and propagate in the shear zone. Usually, the chip

pattern is determined by the combined effects of workpiece properties, cutting conditions and tool geometry [13].

4.3 Tool-Chip Friction Model
Besides the material constitutive model, the friction at the tool-chip interface is also very important in the simulation. The contact between the chip and the tool tends to increase since Inconel 718 is a ductile alloy, which contributes to the cutting force and temperature [8]. Therefore, a better understanding of the friction phenomenon is necessary in order to produce a more realistic cutting simulation [89].

It is noted that various friction models have been researched under different cutting conditions [125–128]. For instance, Haglund et al. [89] developed a friction model based on the Arbitrary-Lagrangian-Eulerian (ALE) approach in metal cutting simulation of hardened steel. Peng et al. [10] found that the friction coefficient in the tool-chip interface decreases with the temperature by using a temperature-dependent friction model. The conventional Coulomb friction model is no longer able to cover all cutting conditions since the tool-chip

contact condition appreciably changes with friction [10]. Therefore, the temperature rises in the chip formation region, and thus the friction coefficient changes. The chip
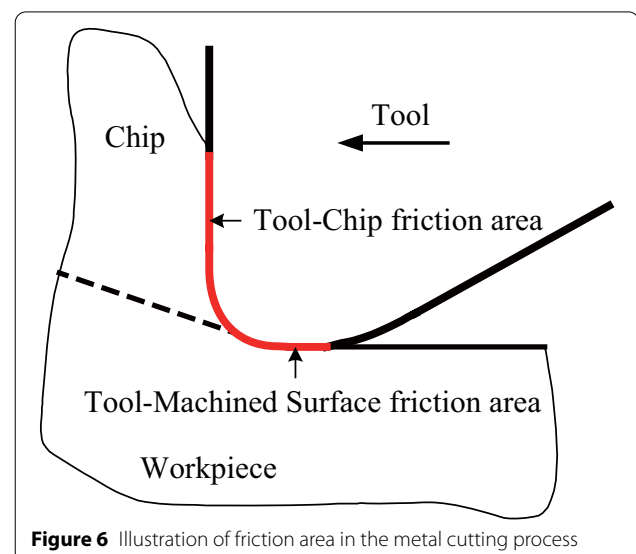

Figure 6 Illustration of friction area in the metal cutting process

Liu *et al. Chin. J. Mech. Eng.* (2021) 34:34

Page 10 of 16

pattern in simulation is also affected by the used friction models [129].

In the metal cutting operations, violent friction exists between the tool and the workpiece. There are mainly two pairs of friction, i.e., the tool-chip friction and the tool-machined surface friction, as shown in Figure 6. The friction at the tool-chip interface significantly influences the frictional force, the normal force and the generated heat, while the friction at the tool-machined surface interface greatly affects the machined surface's roughness, hardness and residual stress. It is has been reported in Ref. [125] that the frictional condition is very complicated at the tool-chip interface and the tool-machined surface interface. Therefore, it is a challenge, due to the uncertainties in metal cutting process, to set up a good friction model as close as the realistic friction when conducting cutting simulation [130].

For the contact between the chip and the tool rake face, Zorev [131] divided the tool-chip interface into a sticking area and a sliding area. Figure 7 shows the distribution of the normal stress and friction stress acting on the tool rake face. In the sticking zone, it is considered that the shear stress is a fixed value, which is equal to the yield stress of the material. In the sliding zone, the friction coefficient μ is a constant in accordance with the Coulomb friction model [99]. In the process of metal cutting simulation, researchers generally use this friction model. According to Zorev's friction model [131], the normal stress initially is the maximum value at the tool tip, and gradually reduces and tends to zero once the chip separates from the tool rake face.

It is reported in Ref. [131] that the distribution of friction shearing stress is more complex than the normal stress. The relation between the normal stress and

the shear stress can be expressed by the following equation [131]:

$$\tau = \begin{cases} \mu\sigma, & \mu\sigma < \tau_{\max}, \text{ sliding area,} \\ \tau_{\max}, & \mu\sigma \geq \tau_{\max}, \text{ sticking area,} \end{cases} \quad (4)$$

where τ is the shear stress, and $\tau_{\max}$ is the maximum equivalent shear stress. σ is the normal stress acting on the interface, and μ is the friction coefficient.

Eq. (4) indicates that the friction at the tool-chip interface is the result of the weight between the normal stress σ and the shear stress τ via fiction coefficient μ. Sliding happens when the shear stress is smaller than $\tau_{\max}$, and sticking stands out when the shear stress is equal to or larger than $\tau_{\max}$ regardless of the normal stress.

5 Experimental Observation

Chip morphology is an important evaluation index of the metal's machinability and cutting characteristics, and it is relevant to the cutting force, machined surface quality and temperature. The trend and final aim of metal cutting is to achieve high material removal rates and thus to realize the automation of the machining operations [132]. This needs reliable cutting process with improvements in surface finish, workpiece accuracy and tool life [133]. To obtain reliable cutting, much attention needs to focus on producing desired type of chip that is easy to be removed. Because the mechanism of chip formation and breaking are both greatly important in machining. Problems related to surface finish, workpiece accuracy and tool life may caused by a minor crack in the chip formation process, especially in high speed machining where detrimental effect tends to be magnified during the undesirable chip formation process [20, 134–139]. Scientific methods to analyze the chip formation mechanism is shown in Figure 8. Usually, the analysis procedure is as follows. Firstly, a chip formation model is proposed based on chip morphology to cover the chip patterns. Then, chips are quantitatively analyzed with a statistical method to know the effects of cutting parameters and tool geometry.

The chip morphology of Inconel 718 and other difficult-to-cut metals will significantly change under various cutting parameters. For instance, Ye et al. [34] observed that the intensity of chip serration increases with the cutting speed in machining of nickel alloy Inconel 718, titanium alloy Ti-6Al-4V, AISI 4340 steel and aluminum alloy 7075. Ozel and Ulutan [83] observed that chip segmentation degree of nickel-based superalloy Inconel 100 will be increased at high feeds and cutting speeds, and it is dominated by the increase of feed. Thellaputta et al. [6] concluded that the chip segmentation of the nickel alloy can be enhanced by using the rhomboid shaped
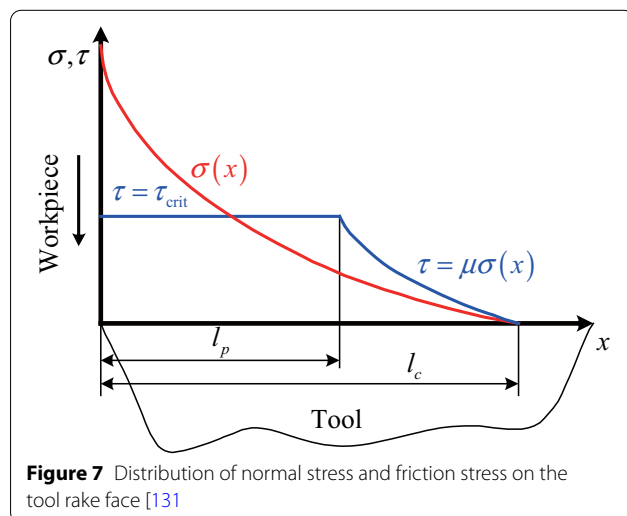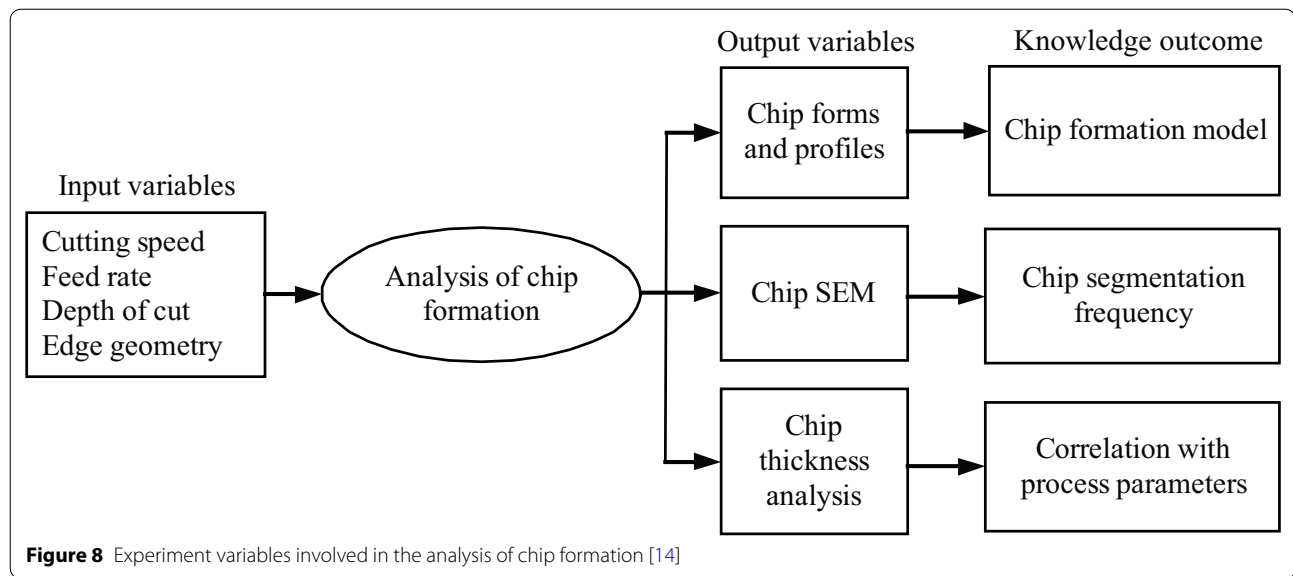

Figure 7 Distribution of normal stress and friction stress on the tool rake face [131]

Liu *et al. Chin. J. Mech. Eng.*   (2021) 34:34

Page 11 of 16

Figure 8 Experiment variables involved in the analysis of chip formation [14]

inserts with relatively great approach angle. Moreover, Li et al. [91] observed that the free surface of the chip shows a serrated lamella pattern in high-speed dry milling of Ti-6Al-4V, and the segmentation degree increases with the cutting speed, feed and depth of cut. Barry et al. [137] found that the increase of the uncut chip thickness and the cutting speed results in a transition from aperiodic to periodic saw-tooth chip formation in machining of Ti-6Al-4V. However, Liu and Su [140] found that the saw-tooth chip pattern of AerMet 100 steel evolves with cutting speed from the white-layered shear bands to the cracked shear bands, and it appears the changes from relatively large separated segments to small and irregular separated segments, and finally to very small grains. Wang and Liu [15] observed that the microstructure of the chip's free surface of the hardened AISI 1045 steel and 7050-T7451 aluminum alloy evolves from lamellae to folds and then to dimples at different combinations of cutting speed and feed.

For most metals, the chip pattern changes at various cutting conditions, especially with the increase of cutting speed. Generally, the evolution of chip types is the following three patterns, i.e., the continuous chip, the serrated chip and the discontinuous chip [22, 36]. The onset of chip serration determined by the cutting speed has been researched for nickel alloy Inconel 718, titanium alloy Ti-6Al-4V, AISI 4340 steel and aluminum alloy 7075 [34]. The chip pattern changes from the continuous pattern to the serrated form at the critical cutting speed (CCS), and highly concentrated shear bands are formed within the serrated chips. As cutting speed further increases, microcracks grow up within the shear localized bands. At still higher cutting speeds, the continuous chip with

saw-tooth edge at the free side is broken into individual segments, i.e., the discontinuous chip [140].

It is known that, metal cutting is a process influenced by many factors. The machining of Inconel 718 involves shear instability that leads to intensely localized deformation [18]. A minor change in chip formation process may give rise to problems related to cutting force variation, rapid tool wear and degradation of the machined surface [132]. It is also known that the saw-tooth chip formation mechanism can be explained by the adiabatic shear theory [19, 42, 137, 141] or the periodic crack theory [75–77]. According to these two theories, the adiabatic shear theory can explain the chip serration at CCS of plastic materials because there is no crack observed within the concentrated shear bands [42, 137], while the periodic crack theory suggests that brittle material tends to produce saw-tooth chips [76], in which the cracks within the concentrated shear band are obvious. However, for Inconel 718, cracks initiating from the saw-tooth edge within shear bands tend to emerge at high cutting speeds. This may be caused by the change of workpiece properties at high cutting speeds having phase transition. Unfortunately, the variations of material properties with cutting speed increasing, and consequently, the influences of the changes on chip formation both were not researched.

Many researches have been done by turning, drilling and milling to investigate the chip formation mechanism of Inconel 718. For example, Shaw and Vyas [76] observed the aperiodic and periodic saw-tooth chips in milling. Komanduri et al. [22], and Komanduri and Brown [29] researched chip segmentation and shear instability in the chip formation process. It is understood

Liu *et al. Chin. J. Mech. Eng.* (2021) 34:34

Page 12 of 16

that the shear localization of Inconel 718 is mainly influenced by cutting speed [17, 142]. Therefore, when cutting speed crosses a critical value, shear-localized chip appears. However, the chips are continuous when cutting speed is below this critical value [143]. As cutting speed continuously increases to a high level, high temperature concentrates in the cutting zone, which causes ductility of workpiece material that may explain the emergence of cracks within shear bands at high cutting speeds. Thus, long and continuous chips with saw-tooth edge at the free side are produced [14, 144]. But at still higher cutting speeds, discontinuous chips are produced [145]. Therefore, a thorough understanding of the machining of Inconel 718, especially at high cutting speeds, is important for improving part quality, tool life and the overall product cost [18].

6 Conclusions

(1) At high cutting speeds, due to the unique properties, Inconel 718 tends to produce the serrated or segmented chips that lead to shear instability in the cutting process. Therefore, conservative cutting parameters are usually employed in actual cutting. In order to improve efficiency and effectiveness, extensive investigations on the mechanism of the chip formation have been carried out.

(2) One the one side, the serrated or segmented chips are favored for the automation of machining operations and the other applications involving chip recycling because they are easy to break. On the other side, chip serration or segmentation is also believed to be a strong incentive to the periodic variation of cutting force, which is correlated with the increased tool wear, the degraded surface finish and the reduced part accuracy. Therefore, the causes and effects of chip serration or segmentation have been placed much attention in order to select the optimal cutting conditions to improve product quality and then to increase tool life.

(3) Failure occurs when the critical damage value is reached. To define a proper damage value for the criterion of chip separation is not easy due to the difficult in experimental measurement or selection. It is believed that the segmented chips are produced when the cutting speed is larger than the critical value. Although insights into this process have been researched extensively, they were mostly dependent on some simplified assumptions. Furthermore, they do not take into consideration of other features such as phase transformation.

(4) Discontinuous chips are also produced at enough high cutting speeds in hard machining in order to get high product efficiency. However, efforts have been mostly placed on dealing with the shear-localized chip formation mechanism such as the adiabatic shear formation and the periodic crack propagation. The discontinuous chip formation process during very high cutting speeds has not been modeled. Consequently, the discontinuous chip formation mechanism has not been fully understood.

(5) The mechanisms related to chip formation in the metal cutting process are complicated, and they are associated with interfacial friction, heat generation, strain and stress in the chip formation region. The metal cutting process is a material deformation process that is highly concentrated within a small zone, and thus, theoretical model or experimental means to analyze this process is limited. Therefore, it is difficult to have a clear configuration.

(6) In the past years, the improvement in FEM has made it possible to simulate the cutting process, and thus to better understand the chip formation mechanisms. Although there are many studies on cutting simulations of chip formation, a thorough research of chip segmentation, such as chip segmentation frequency and its correlation with the cutting parameters, is still not available for Inconel 718. In addition, the relevant research of chip morphology with cutting force and surface degradation in high-speed machining of Inconel 718 is also not available.

Authors' Contributions
CL wrote the manuscript; MW was in charge of the whole trial, review and edition; WZ and YY assisted with review. All authors read and approved the final manuscript.

Authors' Information
Chun Liu, is currently a PhD candidate at *School of Mechanical Engineering, Northwestern Polytechnical University, China.*

Min Wan, is currently a professor at *School of Mechanical Engineering, Northwestern Polytechnical University, China.*

Weihong Zhang, is currently a professor at *School of Mechanical Engineering, Northwestern Polytechnical University, China.*

Yun Yang, is currently an associate professor at *School of Mechanical Engineering, Northwestern Polytechnical University, China.*

Liu *et al. Chin. J. Mech. Eng.*   (2021) 34:34

Page 13 of 16

Author Details
¹ School of Mechanical Engineering, Northwestern Polytechnical University, Xi'an 710072, China. ² State IJR Center of Aerospace Design and Additive Manufacturing, Northwestern Polytechnical University, Xi'an 710072, China.

References
[1] I A Choudhury, M A El-Baradie. Machining nickel base superalloys: Inconel 718. *Proceedings of the Institution of Mechanical Engineers, Part B: Journal of Engineering Manufacture*, 1998, 212(3): 195–206.
[2] I A Choudhury, M A El-Baradie. Machinability of nickel-base super alloys: a general review. *Journal of Materials Processing Technology*, 1998, 77(1-3): 278–284.
[3] F Jafarian, S Masoudi, D Umbrello, et al. New strategies for improvement of numerical model accuracy in machining of nickel-based alloy. *Simulation Modelling Practice and Theory*, 2019, 94: 134–148.
[4] E O Ezugwu, Z M Wang, A R Machado. The machinability of nickel-based alloys: a review. *Journal of Materials Processing Technology*, 1999, 86(1-3): 1–16.
[5] E O Ezugwu, I R Pashby. High speed milling of nickel-based superalloys. *Journal of Materials Processing Technology*, 1992, 33(4): 429–437.
[6] G R Thellaputta, P S Chandra Bose, C S P Rao. Machinability of nickel based superalloys: a review. *Materials Today: Proceedings*, 2017, 4(2): 3712–3721.
[7] S Miller. Advanced materials mean advanced engines. *Interdisciplinary Science Reviews*, 1995, 20(4): 117–129.
[8] L N Lopez de lacalle, J Perez, J I Llorente, et al. Advanced cutting conditions for the milling of aeronautical alloys. *Journal of Materials Processing Technology*, 2000, 100(1-3): 1–11.
[9] E A Loria. Recent developments in the progress of superalloy 718. *The Journal of The Minerals, Metals and Materials Society*, 1992, 44(6): 33–36.
[10] B X Peng, T Bergs, F Klocke, et al. An advanced FE-modeling approach to improve the prediction in machining difficult-to-cut material. *The International Journal of Advanced Manufacturing Technology*, 2019, 103: 2183–2196.
[11] S H Chen, S C Su, P C Chang, et al. The machinability of MAR-M247 superalloy. *Advanced Engineering Forum*, 2011, 1: 155–159.
[12] S H Chen, S C Su, C P Kuo, et al. Determination of stress state in chip formation zone when orthogonal machining nickel-based superalloy Inconel 718. *Journal of the Chinese Institute of Engineers*, 2012, 35(6): 747–754.
[13] Y B Guo, D W Yen. A FEM study on mechanisms of discontinuous chip formation in hard machining. *Journal of Materials Processing Technology*, 2004, 155-156: 1350–1356.
[14] R S Pawade, S S Joshi. Mechanism of chip formation in high-speed turning of Inconel 718. *Machining Science and Technology*, 2011, 15(1): 132–152.
[15] B Wang, Z Q Liu. Serrated chip formation mechanism based on mixed mode of ductile fracture and adiabatic shear. *Proceedings of the Institution of Mechanical Engineers, Part B: Journal of Engineering Manufacture*, 2014, 228(2): 181–190.
[16] R Komanduri, T A Schroeder. On shear instability in machining a nickel-iron base superalloy. *Journal of Engineering for Industry*, 1986, 108(2): 93–100.
[17] D G Flom, R Komanduri, M Lee. High-speed machining of metals. *Annual Review of Materials Science*, 1984, 14(1): 231–278.
[18] Z B Hou, R Komanduri. Modeling of thermomechanical shear instability in machining. *International Journal of Mechanical Sciences*, 1997, 39(11): 1273–1314.
[19] R Komanduri, B F Von Turkovich. New observations on the mechanism of chip formation when machining titanium alloys. *Wear*, 1981, 69(2): 179–188.
[20] R Komanduri. Some clarifications on the mechanics of chip formation when machining titanium alloys. *Wear*, 1982, 76(1): 15–34.
[21] R Komanduri, Z B Hou. On thermoplastic shear instability in the machining of a titanium alloy (Ti-6Al-4V). *Metallurgical and Materials Transactions A*, 2002, 33(9): 2995–3010.
[22] R Komanduri, T Schroeder, J Hazra, et al. On the catastrophic shear instability in high-speed machining of an AISI 4340 steel. *Journal of Engineering for Industry*, 1982, 104(2): 121–131.
[23] S L Cai, L H Dai. Suppression of repeated adiabatic shear banding by dynamic large strain extrusion machining. *Journal of the Mechanics and Physics of Solids*, 2014, 73: 84–102.
[24] J Lorentzon, N Jarvstrat, B L Josefson. Modelling chip formation of alloy 718. *Journal of Materials Processing Technology*, 2009, 209(10): 4645–4653.
[25] Z P Wan, Y E Zhu, H W Liu, et al. Microstructure evolution of adiabatic shear bands and mechanisms of saw-tooth chip formation in machining Ti6Al4V. *Materials Science and Engineering: A*, 2012, 531: 155–163.
[26] L E Murr, A C Ramirez, S M Gaytan, et al. Microstructure evolution associated with adiabatic shear bands and shear band failure in ballistic plug formation in Ti-6Al-4V targets. *Materials Science and Engineering: A*, 2009, 516(1-2): 205–216.
[27] C Z Duan, L C Zhang. Adiabatic shear banding in AISI 1045 steel during high speed machining: mechanisms of microstructural evolution. *Materials Science and Engineering: A*, 2012, 532: 111–119.
[28] S L Semiatin, S B Rao. Shear localization during metal cutting. *Materials Science and Engineering*, 1983, 61(2): 185–192.
[29] R Komanduri, R H Brown. On the mechanics of chip segmentation in machining. *Journal of Engineering for Industry*, 1981, 103(1): 33–51.
[30] A Vyas, M C Shaw. Mechanics of saw-tooth chip formation in metal cutting. *Journal of Manufacturing Science and Engineering*, 1999, 121(2): 163–172.
[31] A Gatto, L Iuliano. Chip formation analysis in high speed machining of a nickel base superalloy with silicon carbide whisker-reinforced alumina. *International Journal of Machine Tools and Manufacture*, 1994, 34(8): 1147–1161.
[32] H Schulz, T Moriwaki. High-speed machining. *CIRP Annals*, 1992, 41(2): 637–643.
[33] D G Thakur, B Ramamoorthy, L Vijayaraghavan. Study on the machinability characteristics of superalloy Inconel 718 during high speed turning. *Materials and Design*, 2009, 30(5): 1718–1725.
[34] G G Ye, Y Chen, S F Xue, et al. Critical cutting speed for onset of serrated chip flow in high speed machining. *International Journal of Machine Tools and Manufacture*, 2014, 86: 18–33.
[35] Y Liu, M Agmell, D D Xu, et al. Numerical contribution to segmented chip effect on residual stress distribution in orthogonal cutting of Inconel 718. *The International Journal of Advanced Manufacturing Technology*, 2020, 109(3-4): 993–1005.
[36] S Sun, M Brandt, M S Dargusch. Characteristics of cutting forces and chip formation in machining of titanium alloys. *International Journal of Machine Tools and Manufacture*, 2009, 49(7-8): 561–568.
[37] M Agmell, V Bushlya, S V A Laakso, et al. Development of a simulation model to study tool loads in pcBN when machining AISI 316L. *The International Journal of Advanced Manufacturing Technology*, 2018, 96(5-8): 2853–2865.
[38] G S Su, Z Q Liu, L Li, et al. Influences of chip serration on micro-topography of machined surface in high-speed cutting. *International Journal of Machine Tools and Manufacture*, 2015, 89: 202–207.
[39] T Mabrouki, F Girardin, M Asad, et al. Numerical and experimental study of dry cutting for an aeronautic aluminium alloy (A2024-T351). *International Journal of Machine Tools and Manufacture*, 2008, 48(11): 1187–1197.
[40] Y Yang, W H Zhang, Y C Ma, et al. An efficient decomposition-condensation method for chatter prediction in milling large-scale thin-walled structures. *Mechanical Systems and Signal Processing*, 2019, 121: 58–76.
[41] V Upadhyay, P K Jain, N K Mehta. Modelling and experimental study of chip serration frequency in dry turning of Ti-6Al-4V alloy. *International Journal of Machining and Machinability of Materials*, 2012, 12(4): 358–371.
[42] M A Davies, Y Chou, C J Evans. On chip morphology, tool wear and cutting mechanics in finish hard turning. *CIRP Annals*, 1996, 45(1): 77–82.
[43] M Bakkal, A J Shih, R O Scattergood. Chip formation, cutting forces, and tool wear in turning of Zr-based bulk metallic glass. *International Journal of Machine Tools and Manufacture*, 2004, 44(9): 915–925.

[44] C Liu, J Sun, Y L Li, et al. Investigation on the milling performance of tita-nium alloy thin-walled part with air jet assistance. *The International Journal of Advanced Manufacturing Technology*, 2018, 95(5-8): 2865–2874.

[45] R F Recht. Catastrophic thermoplastic shear. *Journal of Applied Mechanics*, 1964, 31(2): 189–193.

[46] D M Turley, E D Doyle, S Ramalingam. Calculation of shear strains in chip formation in titanium. *Materials Science and Engineering*, 1982, 55(1): 45–48.

[47] H R Conaway. Machining the high-nickel alloys. *Influence of Metallurgy on Machinability, American Society for Metals*, 1975: 247–256.

[48] G G Ye, S F Xue, M Q Jiang, et al. Modeling periodic adiabatic shear band evolution during high speed machining Ti-6Al-4V alloy. *International Journal of Plasticity*, 2013, 40: 39–55.

[49] G Sutter, G List. Very high speed cutting of Ti-6Al-4V titanium alloy-change in morphology and mechanism of chip formation. *International Journal of Machine Tools and Manufacture*, 2013, 66: 37–43.

[50] A Gente, H W Hoffmeister, C J Evans. Chip formation in machining Ti6Al4V at extremely high cutting speeds. *CIRP Annals*, 2001, 50(1): 49–52.

[51] G G Ye, S F Xue, W Ma, et al. Cutting AISI 1045 steel at very high speeds. *International Journal of Machine Tools and Manufacture*, 2012, 56: 1–9.

[52] V I Babitsky, A V Mitrofanov, V V Silberschmidt. Ultrasonically assisted turning of aviation materials: simulations and experimental study. *Ultrasonics*, 2004, 42(1-9): 81–86.

[53] C Nath, M Rahman. Effect of machining parameters in ultrasonic vibration cutting. *International Journal of Machine Tools and Manufacture*, 2008, 48(9): 965–974.

[54] Y He, Z M Zhou, P Zou, et al. Study of ultrasonic vibration-assisted thread turning of Inconel 718 superalloy. *Advances in Mechanical Engineering*, 2019, 11(10): 1–12.

[55] R Muhammad, M S Hussain, A Maurotto, et al. Analysis of a free machining $\alpha + \beta$ titanium alloy using conventional and ultrasonically assisted turning. *Journal of Materials Processing Technology*, 2014, 214(4): 906–915.

[56] C B Ni, L D Zhu, C F Liu, et al. Analytical modeling of tool-workpiece contact rate and experimental study in ultrasonic vibration-assisted milling of Ti-6Al-4V. *International Journal of Mechanical Sciences*, 2018, 142-143: 97–111.

[57] M R Ibrahim, N H Rafai, E A Rahim, et al. An investigation of cutting mechanics in 2 dimensional ultrasonic vibration assisted milling toward chip thickness and chip formation. *IOP Conference Series: Materials Science and Engineering*, 2015, 100: 012057.

[58] D V Patil, S Ghosh, A Ghosh, et al. On grindability of Inconel 718 under high efficiency deep grinding by monolayer cBN wheel. *International Journal of Abrasive Technology*, 2007, 1(2): 173–186.

[59] S S Li, Y B Wu, M Nomura. Effect of grinding wheel ultrasonic vibration on chip formation in surface grinding of Inconel 718. *The International Journal of Advanced Manufacturing Technology*, 2016, 86(1-4): 1113–1125.

[60] J Y Zhao, Y C Fu, J H Xu, et al. Forces and chip morphology of nickel-based superalloy Inconel 718 during high speed grinding with single grain. *Key Engineering Materials*, 2014, 589-590: 209–214.

[61] Y Peng, Z Liang, Y Wu, et al. Characteristics of chip generation by verti-cal elliptic ultrasonic vibration-assisted grinding of brittle materials. *The International Journal of Advanced Manufacturing Technology*, 2012, 62(5-8): 563–568.

[62] H D Tesfay, Z G Xu, Z C Li. Ultrasonic vibration assisted grinding of bio-ceramic materials: an experimental study on edge chippings with Hertzian indentation tests. *The International Journal of Advanced Manufacturing Technology*, 2016, 86(9-12): 3483–3494.

[63] H Kitzig-Frank, T Tawakoli, B Azarhoushang. Material removal mecha-nism in ultrasonic-assisted grinding of Al_2O_3 by single-grain scratch test. *The International Journal of Advanced Manufacturing Technology*, 2017, 91(9-12): 2949–2962.

[64] N He, T C Lee, W S Lau, et al. Assessment of deformation of a shear localized chip in high speed machining. *Journal of Materials Processing Technology*, 2002, 129(1-3): 101–104.

[65] A Priyadarshini, S K Pal, A K Samantaray. Finite element modeling of chip formation in orthogonal machining. In: *Statistical and Computational Techniques in Manufacturing*, Springer, Berlin, Heidelberg, 2012: 101–144.

[66] G Sutter. Chip geometries during high-speed machining for orthogonal cutting conditions. *International Journal of Machine Tools and Manufacture*, 2005, 45(6): 719–726.

[67] C Z Duan, M J Wang, J Z Pang, et al. A calculational model of shear strain and strain rate within shear band in a serrated chip formed dur-ing high speed machining. *Journal of Materials Processing Technology*, 2006, 178(1-3): 274–277.

[68] M Barge, H Hamdi, J Rech, et al. Numerical modelling of orthogonal cutting: influence of numerical parameters. *Journal of Materials Process-ing Technology*, 2005, 164-165: 1148–1153.

[69] S P Timothy, I M Hutchings. The structure of adiabatic shear bands in a titanium alloy. *Acta Metallurgica*, 1985, 33(4): 667–676.

[70] S P Timothy. The structure of adiabatic shear bands in metals: a critical review. *Acta Metallurgica*, 1987, 35(2): 301–306.

[71] S S Joshi, N Ramakrishnan, P Ramakrishnan. Micro-structural analysis of chip formation during orthogonal machining of Al/SiCp composites. *Journal of Engineering Materials and Technology*, 2001, 123(3): 315–321.

[72] A Molinari, C Musquar, G Sutter. Adiabatic shear banding in high speed machining of Ti-6Al-4V: experiments and modeling. *International Journal of Plasticity*, 2002, 18(4): 443–459.

[73] J Hua, R Shivpuri. Prediction of chip morphology and segmentation during the machining of titanium alloys. *Journal of Materials Processing Technology*, 2004, 150(1-2): 124–133.

[74] G Poulachon, A Moisan. A contribution to the study of the cutting mechanisms during high speed machining of hardened steel. *CIRP Annals*, 1998, 47(1): 73–76.

[75] M A Elbestawi, A K Srivastava, T I El-Wardany. A model for chip forma-tion during machining of hardened steel. *CIRP Annals*, 1996, 45(1): 71–76.

[76] M C Shaw, A Vyas. Chip formation in the machining of hardened steel. *CIRP Annals-Manufacturing Technology*, 1993, 42(1): 29–33.

[77] K Nakayama, M Arai, T Kanda. Machining characteristics of hard materi-als. *CIRP Annals*, 1988, 37(1): 89–92.

[78] Y L Bai, B Dodd. *Adiabatic shear localization: occurrence, theories and applications*. Pergamon Press, Oxford, 1992.

[79] J Barry, G Byrne. The mechanisms of chip formation in machining hardened steels. *Journal of Manufacturing Science and Engineering*, 2002, 124(3): 528–535.

[80] J Y Sheikh-Ahmad, V Quarless, J A Bailey. On the role of microcracks on flow instability in low speed machining of CP titanium. *Machining Science and Technology*, 2004, 8(3): 415–430.

[81] M G Stevenson, P L B Oxley. High temperature stress-strain proper-ties of a low-carbon steel from hot machining tests. *Proceedings of the Institution of Mechanical Engineers*, 1973, 187(1): 263–272.

[82] B Wang, Z Q Liu, Q B Yang. Investigations of yield stress, fracture toughness, and energy distribution in high speed orthogonal cutting. *International Journal of Machine Tools and Manufacture*, 2013, 73: 1–8.

[83] T Ozel, D Ulutan. Effects of machining parameters and tool geometry on serrated chip formation, specific forces and energies in orthogonal cutting of nickel-based super alloy Inconel 100. *Proceedings of the Insti-tution of Mechanical Engineers, Part B: Journal of Engineering Manufacture*, 2013, 228(7): 673–686.

[84] A Molinari, X Soldani, M H Miguelez. Adiabatic shear banding and scaling laws in chip formation with application to cutting of Ti-6Al-4V. *Journal of the Mechanics and Physics of Solids*, 2013, 61(11): 2331–2359.

[85] A E Bayoumi, J Q Xie. Some metallurgical aspects of chip formation in cutting Ti-6wt.%Al-4wt.%V alloy. *Material Science and Engineering: A*, 1995, 190(1-2): 173–180.

[86] H Zhen-Bin, R Komanduri. On a thermomechanical model of shear instability in machining. *CIRP Annals*, 1995, 44(1): 69–73.

[87] J Q Xie, A E Bayoumi, H M Zbib. Analytical and experimental study of shear localization in chip formation in orthogonal machining. *Journal of Materials Engineering and Performance*, 1995, 4(1): 32–39.

[88] G H Li, M J Wang, C Z Duan. Adiabatic shear critical condition in the high-speed cutting. *Journal of Materials Processing Technology*, 2009, 209(3): 1362–1367.

[89] A J Haglund, H A Kishawy, R J Rogers. An exploration of friction models for the chip-tool interface using an Arbitrary Lagrangian-Eulerian finite element model. *Wear*, 2008, 265(3-4): 452–460.

Liu *et al. Chin. J. Mech. Eng.*   (2021) 34:34

Page 15 of 16

[90] J Shi, C R Liu. On predicting chip morphology and phase transformation in hard machining. *The International Journal of Advanced Manufacturing Technology*, 2006, 27(7-8): 645–654.

[91] A H Li, J Zhao, Y H Zhou, et al. Experimental investigation on chip morphologies in high-speed dry milling of titanium alloy Ti-6Al-4V. *The International Journal of Advanced Manufacturing Technology*, 2012, 62(9-12): 933–942.

[92] A Kortabarria, I Armentia, P Arrazola. Sensitivity analysis of material input data influence on machining induced residual stress prediction in Inconel 718. *Simulation Modelling Practice and Theory*, 2016, 63: 47–57.

[93] M Baker. Finite element simulation of high-speed cutting forces. *Journal of Materials Processing Technology*, 2006, 176(1-3): 117–126.

[94] F Jafarian, H Amirabadi, J Sadri. Integration of finite element simulation and intelligent methods for evaluation of thermo-mechanical loads during hard turning process. *Proceedings of the Institution of Mechanical Engineers, Part B: Journal of Engineering Manufacture*, 2013, 227(2): 235–248.

[95] Y M Arisoy, C S Guo, B Kaftanoglu, et al. Investigations on microstructural changes in machining of Inconel 100 alloy using face turning experiments and 3D finite element simulations. *International Journal of Mechanical Sciences*, 2016, 107: 80–92.

[96] S C Lei, Y Shin, F P Incropera. Material constitutive modeling under high strain rates and temperatures through orthogonal machining tests. *Journal of Manufacturing Science and Engineering*, 1999, 121(4): 577–585.

[97] F Z Wang, J B Zhao, A H Li, et al. Three-dimensional finite element modeling of high-speed end milling operations of Ti-6Al-4V. *Proceedings of the Institution of Mechanical Engineers, Part B: Journal of Engineering Manufacture*, 228(6): 893–902.

[98] G R Johnson, W H Cook. A constitutive model and data for metals subjected to large strains, high strain rates and high temperatures. *Proceedings of the 7th International Symposium on Ballistics*, the Hague, the Netherlands, 1983: 541–548.

[99] M Calamaz, D Coupard, F Girot. A new material model for 2D numerical simulation of serrated chip formation when machining titanium alloy Ti-6Al-4V. *International Journal of Machine Tools and Manufacture*, 2008, 48(3-4): 275–288.

[100] U Andrade, M A Meyers, K S Vecchio, et al. Dynamic recrystallization in high-strain, high-strain-rate plastic deformation of copper. *Acta Metallurgica et Materialia*, 1994, 42(9): 3183–3195.

[101] S H Li, B Hou. Material behavior modeling in machining simulation of 7075-T651 aluminum alloy. *Journal of Engineering Materials and Technology*, 2013, 136(1): 011001.

[102] D J Bammann, M L Chiesa, G C Johnson. Modeling large deformation and failure in manufacturing processes. *Theoretical and Applied Mechanics*, 1996: 359–376.

[103] D J Steinberg, S G Cochran, M W Guinan. A constitutive model for metals applicable at high-strain rate. *Journal of Applied Physics,* 1980, 51(3): 1498–1504.

[104] D Umbrello, S Rizzuti, J C Outeiro, et al. Hardness-based flow stress for numerical simulation of hard machining AISI H13 tool steel. *Journal of Materials Processing Technology*, 2008, 199(1-3): 64–73.

[105] B Haddag, S Atlati, M Nouari, et al. Finite element formulation effect in three-dimensional modeling of a chip formation during machining. *International Journal of Material Forming*, 2010, 3(S1): 527–530.

[106] Y Yang, Y L Ke, H Y Dong. Finite element simulation of high-speed cutting. *Acta Aeronauticaet Astronautica Sinica*, 2006, 27(3): 531–535. (in Chinese)

[107] A Hillerborg, M Modeer, P E Petersson. Analysis of crack formation and crack growth in concrete by means of fracture mechanics and finite elements. *Cement and Concrete Research*, 1976, 6(6): 773–781.

[108] Y B Bao, T Wierzbicki. On fracture locus in the equivalent strain and stress triaxiality space. *International Journal of Mechanical Sciences*, 2004, 46(1): 81–98.

[109] T Obikawa, E Usui. Computational machining of titanium alloy-finite element modeling and a few results. *Journal of Manufacturing Science and Engineering*, 1996, 118(2): 208–215.

[110] D J Benson. A mixture theory for contact in multi-material Eulerian formulations. *Computer Methods in Applied Mechanics and Engineering*, 1997, 140(1-2): 59–86.

[111] E G Ng, T I El-Wardany, M Dumitrescu, et al. Physics-based simulation of high speed machining. *Machining Science and Technology*, 2002, 6(3): 301–329.

[112] E Ceretti, M Lucchi, T Altan. FEM simulation of orthogonal cutting: serrated chip formation. *Journal of Materials Processing Technology*, 1999, 95(1-3): 17–26.

[113] L Chuzhoy, R E Devor, S G Kapoor, et al. Machining simulation of ductile iron and its constituents, part 1: estimation of material model parameters and their validation. *Journal of Manufacturing Science and Engineering*, 2003, 125(2): 181–191.

[114] L Chuzhoy, R E Devor, S G Kapoor. Machining simulation of ductile iron and its constituents, part 2: numerical simulation and experimental validation of machining. *Journal of Manufacturing Science and Engineering*, 2003, 125(2): 192–201.

[115] M Baker, J Rosler, C Siemers. A finite element model of high speed metal cutting with adiabatic shearing. *Computers and Structures*, 2002, 80(5-6): 495–513.

[116] T Obikawa, H Sasahara, T Shirakashi, et al. Application of computational machining method to discontinuous chip formation. *Journal of Manufacturing Science and Engineering*, 1997, 119(4B): 667–674.

[117] L C Zhang. On the separation criteria in the simulation of orthogonal metal cutting using the finite element method. *Journal of Materials Processing Technology*, 1999, 89-90: 273–278.

[118] J S Strenkowski, J T Carroll. A finite element model of orthogonal metal cutting. *Journal of Engineering for Industry*, 1985, 107(4): 349–354.

[119] K Komvopoulos, S A Erpenbeck. Finite element modeling of orthogonal metal cutting. *Journal of Engineering for Industry*, 1991, 113(3): 253–267.

[120] Z C Lin, S Y Lin. A coupled finite element model of thermo-elastic-plastic large deformation for orthogonal cutting. *Journal of Engineering Materials and Technology*, 1992, 114(2): 218–226.

[121] K Watanabe, Y Umezu. Cutting simulation using LS-DYNA3D. *Proceedings of the 3rd International LS-DYNA3D Conference*, Kyoto, Japan, 1995.

[122] S I Oh, C C Chen, S Kobayashi. Ductile fracture in axisymmetric extrusion and drawing - part 2: workability in extrusion and drawing. *Journal of Engineering for Industry*, 1979, 101(1): 36–44.

[123] G R Johnson, W H Cook. Fracture characteristics of three metals subjected to various strains, strain rates, temperatures and pressures. *Engineering Fracture Mechanics*, 1985, 21(1): 31–48.

[124] J W Hancock, A C Mackenzie. On the mechanisms of ductile failure in high-strength steels subjected to multi-axial stress-states. *Journal of the Mechanics and Physics of Solids*, 1976, 24(2-3): 147–169.

[125] T Ozel. The influence of friction models on finite element simulations of machining. *International Journal of Machine Tools and Manufacture*, 2006, 46(5): 518–530.

[126] H Puls, F Klocke, D Lung. Experimental investigation on friction under metal cutting conditions. *Wear*, 2014, 310(1-2): 63–71.

[127] J Rech, P J Arrazola, C Claudin, et al. Characterisation of friction and heat partition coefficients at the tool-work material interface in cutting. *CIRP Annals*, 2013, 62(1): 79–82.

[128] F Zemzemi, J Rech, W Ben Salem, et al. Identification of friction and heat partition model at the tool-chip-workpiece interfaces in dry cutting of an Inconel 718 alloy with CBN and coated carbide tools. *Advances in Manufacturing Science and Technology*, 2014, 38(1): 5–22.

[129] Y C Zhang, J C Outeiro, T Mabrouki. On the selection of Johnson-Cook constitutive model parameters for Ti-6Al-4V using three types of numerical models of orthogonal cutting. *Procedia CIRP*, 2015, 31: 112–117.

[130] S B Yang, J H Xu, Y C Fu, et al. Finite element modeling of machining of hydrogenated Ti-6Al-4V alloy. *The International Journal of Advanced Manufacturing Technology*, 2012, 59(1-4): 253–261.

[131] N N Zorev. Inter-relationship between shear processes occurring along tool face and shear plane in metal cutting. *International Research in Production Engineering, ASME*, New York, 1963: 42–49.

[132] I S Jawahir, C A van Luttervelt. Recent developments in chip control research and applications. *CIRP Annals*, 1993, 42(2): 659–693.

[133] Y Ning, M Rahman, Y S Wong. Investigation of chip formation in high speed end milling. *Journal of Materials Processing Technology*, 2001, 113(1-3): 360–367.

Liu *et al. Chin. J. Mech. Eng.*   (2021) 34:34

Page 16 of 16

[134] A Banerjee, H Y Feng, E V Bordatchev. Geometry of chip formation in circular end milling. *The International Journal of Advanced Manufacturing Technology*, 2012, 59(1-4): 21–35.

[135] M Cotterell, G Byrne. Characterisation of chip formation during orthogonal cutting of titanium alloy Ti-6Al-4V. *CIRP Journal of Manufacturing Science and Technology*, 2008, 1(2): 81–85.

[136] R Shivpuri, J Hua, P Mittal, et al. Microstructure-mechanics interactions in modeling chip segmentation during titanium machining. *CIRP Annals*, 2002, 51(1): 71–74.

[137] J Barry, G Byrne, D Lennon. Observations on chip formation and acoustic emission in machining Ti-6Al-4V alloy. *International Journal of Machine Tools and Manufacture*, 2001, 41(7): 1055–1070.

[138] M Cotterell, G Byrne. Dynamics of chip formation during orthogonal cutting of titanium alloy Ti-6Al-4V. *CIRP Annals*, 2008, 57(1): 93–96.

[139] T Obikawa, M Anzai, T Egawa, et al. High speed machining: a review from a viewpoint of chip formation. *Advanced Materials Research*, 2011, 188: 578–583.

[140] Z Q Liu, G S Su. Characteristics of chip evolution with elevating cutting speed from low to very high. *International Journal of Machine Tools and Manufacture*, 2012, 54-55: 82–85.

[141] R F Recht. A dynamic analysis of high-speed machining. *Journal of Engineering for Industry*, 1985, 107(4): 309–315.

[142] R M Arunachalam, M A Mannan, A C Spowage. Surface integrity when machining age hardened Inconel 718 with coated carbide cutting tools. *International Journal of Machine Tools and Manufacture*, 2004, 44(14): 1481–1491.

[143] H K Toenshoff, H Winkleri, M Patzke. Chip formation at high-cutting speeds. *American Society of Mechanical Engineers, Production Engineering Division*, 1984: 95–100.

[144] E O Ezugwu, S H Tang. Surface abuse when machining cast iron (G-17) and nickel-base superalloy (Inconel 718) with ceramic tools. *Journal of Materials Processing Technology*, 1995, 55(2): 63–69.

[145] A Devillez, F Schneider, S Dominiak, et al. Cutting forces and wear in dry machining of Inconel 718 with coated carbide tools. *Wear*, 2007, 262(7-8): 931–942.